Position-space gluon propagator from quenched lattice QCD

Feliciano de Soto[1,*]

[1]Departamento de Sistemas Físicos, Químicos y Naturales. Universidad Pablo de Olavide. Ctra. Utrera km 1. 41013 Sevilla (Spain)

Abstract.
We report novel lattice QCD results for the position-space gluon propagator in Landau gauge from quenched simulations. Using standard Wilson action, we computed gluon propagator in position space with a detailed treatment of hypercubic errors. Gluon propagator is scrutinized in position-space, discussing on the usefulness of the long-distance behavior of gluon propagator for constraining the gluon spectral function or the deep infrared running of the gluon propagator in momentum-space.

1 Introduction

Despite the fact that without quarks, Quantum Chromodynamics (QCD) is scale invariant, i.e., the Lagrangian of the theory that describe gluon interactions (or Yang-Mills Lagrangian) does not include any mass-scale, hadrons acquire a mass due to gluon interactions which is responsible for most of the observable mass in the universe and whose description requires the use of non-perturbative methods such as lattice-QCD or Schwinger-Dyson Equations [1].

Among the non-perturbative features of Yang-Mills theories, the study of the infrared behavior of the fundamental Green's functions such as gluon or ghost propagators has remained as an interesting topic during the last decades, in connection with, for example, confinement scenarios such as Kugo-Ojima or Gribov-Zwanziger [2–5]. In particular, momentum-space gluon propagator has attracted a lot of attention since the early days of lattice-QCD [6] in relation to the emergence of a dynamically generated gluon mass. Over the the last decade a noticeable consensus has been achieved over the fact that gluon propagator has a finite value at zero momentum, both from lattice [7–11] and Dyson-Schwinger equations (see [12] and references therein). Another interesting feature of the gluon propagator is that it is known to violate positivity [13, 14], a fact that can be understood as a signature of gluons being confined as stated by Osterwalder and Schrader [15, 16] axiom for Euclidean quantum field theories.

The lattice calculation of any Green function is known to be affected by discretization and finite-volume errors. A particular kind of lattice error that is associated to the fact that the hypercubic lattice discretization of space-time (and correspondingly its Fourier reciprocal space) breaks rotational invariance, the so-called H4 errors [17]. These errors have been widely studied in momentum-space, while in position-space, on the contrary, very little is known about the effects of breaking rotational invariance. In this paper, we will apply the

*e-mail: fcsotbor@upo.es

generalized H4-extrapolation method in [18] to the position-space gluon propagator. Finally, we will discuss the phenomenological relevance of the position-space propagator, as positivity violation of gluon propagator. Direct calculations of gluon propagator in position space $\Delta(x)$ would show a direct evidence of positivity violation, and will be presented in this note together with that of the momentum-space.

2 Landau-gauge gluon propagator and hypercubic errors

We have generated 2000 quenched gauge field configurations using standard Wilson action for $\beta = 5.6$, 5.7, 5.8, 6.0 and 6.2 for 32^4 lattice sites and 500 configurations for $\beta = 5.6$ and 5.8 and 48^4 lattice sites. Details on the action used and Landau gauge fixing algorithm can be found in [19, 20]. The lattice spacing for $\beta = 6.0$ ($a_{\beta=6.0} = 0.096 fm$) has been taken from Ref. [21] while for the rest, the relative calibration method presented in [22] has been used., thus obtaining $a_{\beta=5.6} = 0.237 fm$, $a_{\beta=5.7} = 0.182 fm$, $a_{\beta=5.8} = 0.144 fm$, and $a_{\beta=6.2} = 0.070 fm$.

In Landau gauge, the bare gluon propagator in momentum space is obtained from the two-point correlation function $\langle \widetilde{A}^a_\mu(q) \widetilde{A}^b_\nu(-q)\rangle$ where $\langle \cdots \rangle$ represents the Monte Carlo average over field configurations and $A^a_\mu(q)$ stands for SU(3) gauge fields in Fourier-space with color index a, Lorentz index α and momentum q that are obtained from the discrete Fourier transform of the gauge fields in position-space $A^a_\mu(x)$. In Landau gauge they satisfy $\partial_\mu A^a_\mu(x) = 0$ or, in momentum-space, they must be transverse, i.e., $q_\mu \widetilde{A}^a_\mu(q) = 0$. The scalar form-factor of the gluon propagator in momentum-space is then:

$$\Delta_0(q) = \frac{1}{24} \langle \widetilde{A}^a_\mu(q) \widetilde{A}^a_\mu(-q)\rangle \,. \tag{1}$$

In position-space, the diagonal contribution to the propagator is obtained as:

$$\Delta_0(x) = \frac{1}{24N^4} \sum_y \langle A^a_\mu(y) A^a_\mu(y-x)\rangle \,. \tag{2}$$

It is interesting to note that $\Delta_0(x)$ is the inverse discrete Fourier transform of $\Delta_0(q)$:

$$\Delta_0(x) = \frac{1}{24L^4} \sum_y \sum_{q,q'} e^{-iqy} e^{-iq'(y-x)} \langle \widetilde{A}^a_\mu(q) \widetilde{A}^a_\mu(q')\rangle = \sum_q e^{-iqx} \Delta_0(q) \,. \tag{3}$$

2.1 Lattice errors in momentum-space

While in the continuum $\Delta_0(q)$ depends only on q^2 (resp x^2 for the position-space case), the lattice breaks rotational invariance and the propagator acquires a dependence in the lattice H(4) group invariants $q^{[4]}$, $q^{[6]}$ and $q^{[8]}$, where $q^{[2n]} = \sum_{\mu=1}^4 q_\mu^{2n}$. This is a spurious dependence that should disappear in the limits of zero lattice spacing (continuum limit) and infinite volume (thermodynamic limit). It produces different values of the propagator for the same q^2 if the momenta are not related by H(4) symmetry. In momentum-space, this type of discretization error is responsible for the known half-fishbone structure observed in gluon or quark propagators when one considers all the lattice momenta [23–26]. Different strategies have been employed to minimise the impact of these hypercubic errors on the lattice propagators such as making a diagonal cut on the momenta [27] or using a tree-level correction [26, 28]. Here, we will use the methods based in using the spurious dependence on higher order invariants of the H(4) group to recover rotationally invariant propagators [17]. Among the advantages of this method that we will exploit here is that it can be applied in a unified treatment also to position-space propagators [18].

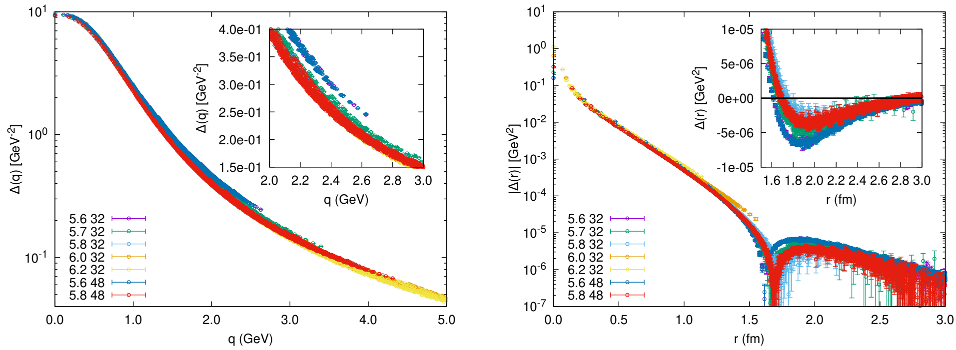

Figure 1. Landau-gauge gluon propagator in momentum (left) and position-space (right) as obtained from the lattice before eliminating lattice errors. The right plot shows the absolute value of the position-space propagator, which has a zero for $r \sim 1.6$ fm (see inset plot).

Keeping only the leading-order invariant $q^{[4]}$, the H4-extrapolation method [18] proposes to recover the rotationally invariant propagator $\widetilde{\Delta}(q^2)$ as

$$\widetilde{\Delta}_0(q^2) = \widetilde{\Delta}_0(q^2, q^{[4]}) \times \left[1 + a^2 c(q^2) \frac{q^{[4]}}{(q^2)^2} \right] \tag{4}$$

where $\widetilde{\Delta}_0(q^2, q^{[4]})$ are the lattice data for all orbits and $c(q^2)$ some unknown function of q^2. The method is based in minimising the quantity:

$$\chi^2 = \sum_{q^2} \sum_{q^{[4]}} \left(\frac{\widetilde{\Delta}_0(q^2) - \widetilde{\Delta}_0(q^2, q^{[4]}) \times \left[1 + a^2 c(q^2) \frac{q^{[4]}}{(q^2)^2} \right]}{\sigma(q^2, q^{[4]})} \right)^2 , \tag{5}$$

varying the values of the propagator at each q^2 once the artifacts have been removed, $\widetilde{\Delta}_0(q^2)$, and the function $c(q^2)$. This minimisation amounts to solving a linear least-squares problem if this function is written as a linear combination of several terms with unknown coefficients, c_i such as:

$$c(q^2) = c_0 + c_1 q^2 + c_2 q^4 \,. \tag{6}$$

Indeed, this is the reason why Eq. (4) is written in this way instead of introducing the correction in the other term of the equation: to make the minimisation a linear least-squares problem.

The application of this method in momentum space leads to a bare propagator with a smooth dependence on q^2 for each a. The renormalized propagator is obtained as the continuum limit:

$$\widetilde{\Delta}_{R,\mu}(q^2) = \lim_{a \to 0} Z_3^{-1}(\mu^2, a) \widetilde{\Delta}_0(q^2, a) \tag{7}$$

with the renormalization condition $\widetilde{\Delta}_{R,\mu}(q^2 = \mu^2) = 1$, and all the lattice artifacts have to disappear once the continuum limit has been taken.

The most extended procedure starts by rescaling the propagators at a given common scale, something that may introduce a bias in the renormalized propagators if some uncorrected discretization errors are present at the scale chosen, as discussed in [20, 22]. Indeed, the naive application of this method pushes the discretization errors to the deep-IR with the rescaling.

Here we will use a different approach and define the renormalized propagator as:

$$\widetilde{\Delta}_{R,\mu}(q^2) = z_a \widetilde{\Delta}_0(q^2, a) \times \left[1 + b_1 a^2 q^2 \right] \times \left[1 + d_1 e^{-d_2 L q} / L \right] \tag{8}$$

where z_β is a lattice spacing dependent normalization constant, and discretization and finite-volume artifacts have been included as multiplicative corrections that depend on the parameters b_1, d_1, and d_2.

In order to fix the values of those parameters, we rely on a parametrization of the renormalized propagator $\widetilde{\Delta}_{R,\mu}(q^2)$ and minimise the quantity:

$$\chi^2 = \sum_{a,q^2} \left(\frac{\widetilde{\Delta}_{R,\mu}(q^2) - z_a \widetilde{\Delta}_0(q^2, a) \times \left[1 + b_1 a^2 q^2 \right] \times \left[1 + d_1 e^{-d_2 L q} / L \right]}{z_a \sigma_(q^2, a)} \right)^2 \tag{9}$$

where the sum is extended to all the lattice data points for all lattice set-ups described above and the parameters to be fixed will be the ones in the parametrization of the renormalized propagator and z_a, b_1, d_1, and d_2 in Eq. (8).

To that aim, we have considered the following parametrizations:

$$\widetilde{\Delta}^{-1}_{R,\mu}(q) = q^2 \left[1 + \left(\kappa_1 - \frac{\kappa_2}{1 + \left(q^2/\kappa_4^2 \right)^2} \right) \log \frac{q^2}{\mu^2} \right] + R(q^2) - R(\mu^2) \tag{10}$$

with $R(q^2)$ a Padé approximant,

$$R(q^2) = \frac{\sigma_0 + \sigma_1 q^2}{1 + q^2/\sigma_2^2 + q^4/\sigma_4^4}. \tag{11}$$

which was used in [29]. In order to check any possible bias introduced in the fit associated to this fitting function, we have repeated the analysis using

$$\widetilde{\Delta}_{R,\mu}(q) = \frac{1}{\mu^2} \left(\frac{\mu^2 + m^2}{q^2 + m^2} \right)^n \frac{R(q^2)}{R(\mu^2)} \tag{12}$$

for $n = 3/2$.

The use of any of those parametrizations at this level is purely instrumental, as the purpose at this stage is to detect the presence of uncorrected O4 discretization or finite-volume errors fixing the values of the parameters b_1, d_1, and d_2 in Eq.(8). With the values of the parameters determined, the continuum, thermodynamic limit of the lattice data will be taken.

The values of the coefficients b_1, d_1, and d_2 obtained when using the fitting functions (10) and (12) are compatible within errors. Finally, combining the results for both fits we obtain: $b_1 = 0.0077(6)$, $d_1 = 3.7(2)$ GeV^{-1} and $d_2 = 0.26(3)$, where the quoted errors have been obtained through Jackknife method. Applying the r.h.s. of Eq.(8) to the lattice data for all data sets, we obtain the gluon propagator depicted in the left panel of Fig.2.

2.2 Lattice errors in position-space

The shape of lattice errors that affect gluon propagator in position-space is a bit more involved than in momentum space, as has been analyzed in detail in [18], where a generalized method for the treatment of the lattice errors in both position and momentum-space was introduced.

We employ a fit similarly to the one sketched in the previous section for position-space, i.e., the dominant H4 error was assumed to be a multiplicative correction of the form,

$$\Delta_0(x^2) = \Delta_0(x^2, x^{[4]}) \times \left[1 + a^2 c(x^2) \left(\frac{x^{[4]}}{(x^2)^2} - \frac{1}{2} \right) \right] \tag{13}$$

with the addition of the $1/2$ as *optimal* value of $\frac{x^{[4]}}{(x^2)^2}$, and the function $c(x^2)$ that in this case dimensional arguments suggest it should behave as $1/x^2$.

Once the H4-errors have been corrected using this method, the remaining O4-errors are treated following a similar strategy to the one used in momentum-space. In this case including only finite-volume terms for large distances, we used:

$$\Delta_{R,\mu}(x^2) = z_a \Delta_0(x^2, a) + d_1' e^{-d_2' x/L}/L^2 \,, \tag{14}$$

with $d_1' = 1.42 \cdot 10^{-2}$ and $d_2' = 5.4$, and our final result for the propagator are presented in Fig. 2(right).

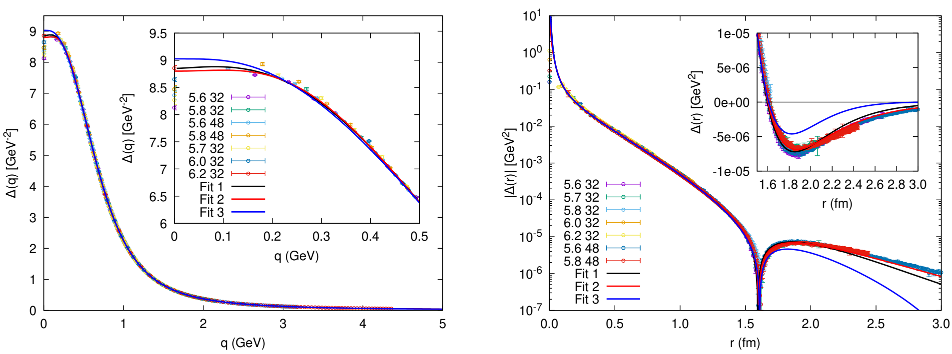

Figure 2. Landau-gauge gluon propagator in momentum (left) and position-space (right) obtained from the lattice after eliminating lattice errors. The three continuum lines in the left plot correspond to the fits discussed in the text, while their counterparts in the right plot are obtained by numerically computing their Fourier transforms.

After the treatment of lattice artifacts, we will make a further check of the methodology followed by numerically computing the Fourier transform of the propagator. To this aim, we have fitted the momentum-space propagator to the phenomenological parametrizations in Eqs.(10-12) introduced in last section. We added a Very Refined Gribov-Zwanziger fit (introduced in [30]), and defined by:

$$\widetilde{\Delta}_{R,\mu}(q) = Z \frac{q^4 + M_2^2 q^2 + M_1^4}{q^6 + M_5^2 q^4 + M_4^4 q^2 + M_3^6} \,. \tag{15}$$

Those three fitting functions will be refered as Fit 1, 2 and 3 respectively, and the results of the fits have been included in the left panel of Fig. 2.

If both position and momentum-space propagators were free of lattice artifacts, $\widetilde{\Delta}(q)$ and $\Delta(x)$ would be related by a Fourier transform. We will perform a continuum Fourier transform:

$$\Delta_{FT}(x) = \frac{1}{4\pi^2 x} \int_0^\infty dq\, q^2 \widetilde{\Delta}(q) J_1(qx) \tag{16}$$

and compare $\Delta_{FT}(x)$ with the lattice propagator in position-space after taking the continuum and thermodynamic limits, $\Delta(x)$. In order to compute the Fourier transform in Eq.(16), a continuum description of $\widetilde{\Delta}(q)$ is needed for $q \in (0, \infty)$. We will use here a somehow different approach to the one presented in [18], and will use the three fitting functions discussed above for the computation of the Fourier transform in Eq.(16). The result has been plotted in the right panel of Fig.2 where also the the lattice data for $\Delta(x)$ are represented. This plot shows a strikingly good agreement between the lattice data in position-space and the inverse Fourier transform of the fitting functions in momentum space, in particular for the Yukawa-like propagator in Eq.(12). It is important to remark that there is no fit in this plot; the agreement being indicative of a proper treatment of lattice artifacts in both position and momentum-space.

3 Positivity violation from gluon propagator

The position-space propagator for a one-particle state with mass m behaves as

$$\Delta(x) \sim \frac{e^{-mx}}{x^{\frac{D-1}{2}}} \tag{17}$$

where D is the dimension of space [31]. Although this behavior reproduces qualitatively well the lattice data for intermediate distances (below $\sim$ 1 fm, according to Fig. 2), the lattice data show unequivocally negative values of the gluon propagator for distances larger than $\sim$ 1.6 fm, signaling positivity violation in gluon-propagator. The fact that both the lattice data in position-space and the inverse Fourier transforms of the fitting functions in momentum-space signal the position of this zero at the same distance make us confident that it is not affected by lattice errors.

If we introduce the spectral density $\rho(\omega)$ as:

$$\widetilde{\Delta}(q) = \int dm \frac{\rho(m)}{q^2 + m^2}\,, \tag{18}$$

after Fourier transform, the position-space propagator results:

$$\Delta(x) = \int dm\, \rho(m)\, K_1(mx)\,, \tag{19}$$

where K_1 stands for the modified Bessel function of the second kind. If the spectral density is non-positive defined, it is said to violate positivity, and as a consequence the particle cannot exist as a propagating particle.

The propagator of a free massive boson in Eq. (17) does not violate positivity, but gluon propagator as obtained from the lattice noticeably deviates from this behavior for large distances, becoming negative and, thus, implying positivity violation. It can be seen from Eq. (19), as $\Delta(x)$ negative requires that $\rho(m)$ cannot be positive for all values of m. In the Zwanziger scenario for confinement [4], positivity violation is manifest as $\widetilde{\Delta}(q^2 = 0) = 0$ implies that $\Delta(x)$ cannot be positively defined. As this scenario is not realized, it is not evident from $\widetilde{\Delta}(q)$ whether gluon violates positivity. From momentum-space gluon propagator, a possible signature of positivity violation would be a non-monotonous behavior of $\widetilde{\Delta}(q^2)$, something that has been recently observed in large-volume lattice data [29], which show indeed that gluon propagator has a maximum at a rather infrared scale located roughly around 150 MeV.

The existence of a zero in the position-space propagator is directly linked to the spectral density $\rho(m)$, and can be used to study the spectral decomposition of the gluon propagator, that has been the object of a series of recent works [32, 33]. The idea of using the position-space propagator to study the spectral density appears already in [34].

Moreover, position-space propagator is intimately linked to the Schwinger function

$$S(t) = \int d^3\vec{x}\, \Delta(\vec{x}, t) = \frac{1}{2\pi} \int dq_0\, \widetilde{\Delta}(\vec{0}, q_0)\, e^{iq_0 t} = \int dm\, \rho(m)\, e^{-mt}\,. \tag{20}$$

From the lattice, this quantity can be efficiently computed via the wall-to-wall correlator [34] which reduces statistic errors. The lattice data for the Schwinger function obtained for the

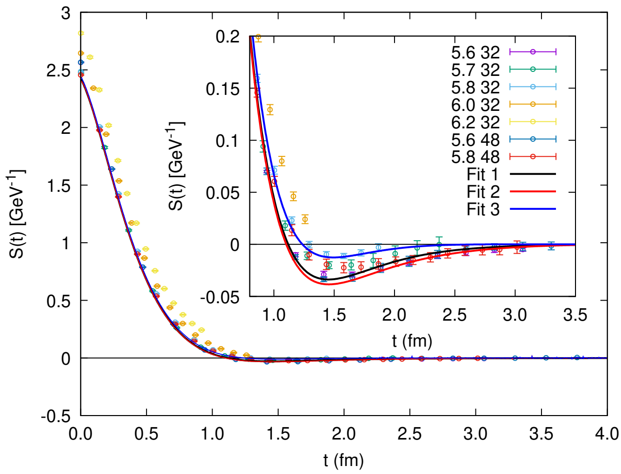

Figure 3. Schwinger function for the different lattice setups and the results of the using the fits made in momentum-space and discussed in section 3 to compute $S(t)$ using Eq. (20). Note that no fit has been done for $S(t)$ and also how the difference among the different lattice setups is larger than in the case of propagators, as a consequence of lattice errors that have not been properly cured.

extensive set of quenched gauge field configurations used in this work have been plotted in Fig. 3. Contrarily to the case of the gluon propagator, the Schwinger function depends only on one space variable, and the H4 method does not provide a way to eliminate the artifacts. A close inspection of the lattice data for the Schwinger function plotted in Fig. 3 shows that the different setups do not scale as well as for the propagator (either in position or momentum-space), and sizable differences among setups with different lattice spacings and volumes exist. In this sense, the use of position or momentum-space propagators allows for a better treatment of lattice errors because of the advantages of the H4 method as well as because there is a larger number of lattice points.

In figure 3, also the value of $S(t)$ obtained when plugging into the definition of Eq. (20) the results of the fits with the functions (10) (12), and (15) for the momentum-space propagator. Both the lattice data (except the smallest lattice volumes) and the continuous functions exhibit a zero-crossing, and positivity violation is manifest from this quantity. Indeed, it is well known that both lattice and Dyson-Schwinger methods predict a zero at around 1.1 fm [14, 35].

4 Conclusions

This note presents an extensive quenched lattice calculation of gluon propagator both in position and momentum-space, with a detailed treatment of lattice artifacts. In particular those due to rotational invariance breaking (H4 errors) but also H4-symmetric ones. By doing so we have obtained smooth and precise propagators $\widetilde{\Delta}(q)$ and $\Delta(x)$ (Fig. 2). We have furthermore introduced a method to validate the extrapolation to the continuum and thermodynamic limit via a numerical Fourier transform of the lattice data. The agreement found between the lattice data in position-space and the inverse Fourier transform of the fitting functions in momentum-space (See Fig. 2) guarantees the validity of the formalism employed.

We have obtained a position-space propagator with very good precision up to distances of ~ 3fm, something that up to the knowledge of the author has never appeared in the literature, most probably due to the impact of H4 errors, for which only the new method presented in [18] allows for a proper treatment. This position-space propagator has a zero for a distance of approximately 1.6fm, being negative beyond this distance, something that can be understood as a signal that gluon is a confined particle. The long distance behavior of the position-space gluon propagator is related to the non-perturbative domain in momentum-space, and it could be used to constrain the complex structure of the spectral density $\rho(m)$.

The Schwinger function $S(t)$ in Eq.(20) has also been computed (Fig. 3), both from the different lattice setups and from the three fitting functions used for the momentum-space propagator. It also exhibits violation of positivity, but the lattice estimate is not as precise as for the propagators, thus, employing the position-space propagator seems more adequate for the studies of positivity violation as well as for the study of the deeply non-perturbative regime of Yang-Mills theories.

Acknowledgments. This work was supported by Spanish research project PID2019-107844-GB-C2 and the regional Andalusian P18-FR-5057. All calculations have been performed at the UPO computing center, C3UPO.

References

[1] C.D. Roberts, Symmetry **12**, 1468 (2020), 2009.04011
[2] T. Kugo, I. Ojima, Progress of Theoretical Physics Supplement **66**, 1 (1979)
[3] V. Gribov, Nuclear Physics B **139**, 1 (1978)
[4] D. Zwanziger, Nuclear Physics B **364**, 127 (1991)
[5] D. Zwanziger, Nuclear Physics, Section B **412**, 657 – 730 (1994)
[6] J. Mandula, M. Ogilvie, Physics Letters B **185**, 127 (1987)
[7] A. Cucchieri, T. Mendes, Phys. Rev. Lett. **100**, 241601 (2008)
[8] A.C. Aguilar, D. Binosi, J. Papavassiliou, Phys. Rev. D **78**, 025010 (2008)
[9] I. Bogolubsky, *et al.*, Physics Letters B **676**, 69 (2009)
[10] O. Oliveira, P.J. Silva, Phys. Rev. D **86**, 114513 (2012)
[11] P. Boucaud, *et al.*, Few Body Syst. **53**, 387 (2012), 1109.1936
[12] M.Q. Huber, Physics Reports **879**, 1 (2020)
[13] A. Cucchieri, T. Mendes, A.R. Taurines, Phys. Rev. D **71**, 051902 (2005)
[14] P.O. Bowman, *et al.*, Phys. Rev. D **76**, 094505 (2007)
[15] K. Osterwalder, R. Schrader, Communications in Mathematical Physics **31**, 83 (1973)
[16] K. Osterwalder, R. Schrader, Communications in Mathematical Physics **42**, 281 (1975)
[17] F. de Soto, C. Roiesnel, JHEP **09**, 007 (2007), 0705.3523
[18] F. de Soto, JHEP **10**, 069 (2022), 2204.12189
[19] A. Ayala, *et al.*, Phys. Rev. D **86**, 074512 (2012), 1208.0795
[20] P. Boucaud, *et al.*, Phys. Rev. D **98**, 114515 (2018), 1809.05776
[21] S. Necco, R. Sommer, Nucl. Phys. B **622**, 328 (2002), hep-lat/0108008
[22] P. Boucaud, *et al.*, Phys. Rev. D **96**, 098501 (2017), 1704.02053
[23] D. Becirevic, *et al.*, Phys. Rev. D **61**, 114508 (2000), hep-ph/9910204
[24] D. Becirevic, *et al.*, Phys. Rev. D **60**, 094509 (1999), hep-ph/9903364
[25] P. Boucaud, *et al.*, Phys. Lett. B **575**, 256 (2003)
[26] F.D.R. Bonnet, *et al.*, Phys. Rev. D **64**, 034501 (2001), hep-lat/0101013
[27] D.B. Leinweber, *et al.*, Phys. Rev. D **60**, 094507 (1999)
[28] M. Constantinou, *et al.*, Journal of High Energy Physics **2009**, 064–064 (2009)
[29] A.C. Aguilar, *et al.*, Phys. Rev. D **104**, 054028 (2021), 2107.00768
[30] D. Dudal, O. Oliveira, P.J. Silva, Annals Phys. **397**, 351 (2018), 1803.02281
[31] G. Parisi, Nucl. Phys. B **180**, 378 (1981)
[32] D. Dudal, O. Oliveira, M. Roelfs, P. Silva, Nucl. Phys. B **952**, 114912 (2020)
[33] D. Binosi, R.A. Tripolt, Phys. Lett. B **801**, 135171 (2020), 1904.08172
[34] T. Iritani, H. Suganuma, H. Iida, Phys. Rev. D **80**, 114505 (2009), 0908.1311
[35] C.S. Fischer, R. Alkofer, Phys. Rev. D **67**, 094020 (2003), hep-ph/0301094